Pergamon

Int. J. Heat Mass Transfer. Vol. 41, No. 1, pp. 117–126, 1998

Printed in Great Britain
0017-9310/98 $19.00+0.00

PII: S0017-9310(97)00088-4

Mathematical model of self-sustaining combustion in inert porous medium with phase change under complex heat transfer

V. V. MARTYNENKO

Chemical Physics Laboratory, Heat and Mass Transfer Institute, Byelorussian Academy of Science, Minsk 220072, Belarus

and

R. ECHIGO and H. YOSHIDA

Department of Mechanical Engineering and Science, Tokyo Institute of Technology, Meguro-ku, Tokyo 152, Japan

(*Received* 10 *May* 1996 *and in final form* 13 *March* 1997)

Abstract—The phenomenon of self-sustaining combustion of a gaseous mixture in inert high porous medium with prior vaporization of liquid droplets is studied by means of a numerical simulation. The complex heat transfer includes convective, conductive and radiative heat transfer between three phases: gas, solid and liquid. Evaporation and different modes of convective heat transfer between liquid, gaseous and solid phases are considered in detail. In particular, the behavior of particles which collide against and deposit on the skeleton of porous medium is taken into account, as well as the dependence of the heat transfer coefficient between liquid and solid on the skeleton superheat. © 1997 Elsevier Science Ltd.

1. INTRODUCTION

Considerable practical benefits from the preheating of a combustible mixture have been pointed out by Weinberg [1], who proposed several recuperative schemes for practice [2]. In these schemes generally unused heat of combustion products was regenerated to the reactants. Practically, the regime of excess enthalpy burning was realized in many types of heat exchangers. Among them the porous material burners have promising industrial applications because of good combustion enhancement performance as reviewed by Echigo [3]. The preliminary radiative heating of combustible mixtures in porous materials extended the limits of self-sustaining combustion of lean fuels. Unique features of gas combustion in a porous medium result in the superadiabaticity phenomenon [4], which means that the gas temperature exceeds the theoretical adiabatic flame temperature in free space. In particular, Hanamura *et al.* [5] theoretically showed that in combustion with reciprocating flow the maximum flame temperature attained in the porous medium is 13 times higher than the adiabatic one in free space. Also, analytical solution for superadiabatic reciprocating flow combustion is proposed to estimate an optimum period of reverse in a limiting case when convective heat transfer is dominant [6]. Under an optimum period of reverse the gas temperature exceeds the theoretical adiabatic flame temperature in free space at the most. On the basis of the applicability to dilute fuels and additional control over various waste products, such combustion has commercial applications for the incineration of organic pollutants [7]. Moreover, applications of reciprocating flow combustion system for advanced power generation are considered by Echigo *et al.* [8], and its combustible limit has been found analytically by Hoffmann *et al.* [9].

On the other hand, the combustion of liquid fuel is widely applied in industrial furnaces. The actual combustion phenomenon for liquid is complicated by different modes of heat exchange including phase change; for example, evaporation rate determines the intensity of heat transfer as well as burning. The problem of liquid droplets has a background based on the theoretical and experimental investigation of vaporization and flaming of liquid droplets [10–13]. In ref. [10], different vaporization models are compared for single droplet and also for spray. The classical droplet vaporization model was re-examined by Abramzon and Siringano [11] in order to develop a model for the spray combustion calculation, which traces the life histories of many individual droplets. Elperin and Krasovitov [12] developed the quasi-steady model of combustion and evaporation of a large and moderate size single droplet in a quiescent atmosphere.

Although past investigations have dealt with droplet combustion of liquid fuel principally in the free

NOMENCLATURE

A	frequency factor for reaction kinetics
c	specific heat at constant pressure
d	diameter of liquid droplet
D	mean size of element of porous material structure
E	activation energy
E_n	exponential integral function of nth order
h	heat transfer coefficient
h_b	heat transfer coefficient between end surface of porous medium and gas
H	combustion heat
I_0, I_c	incident radiation intensity
I_b	blackbody radiation intensity
k	absorption coefficient
L	latent heat of evaporation
$\dot{M}_f$	evaporation rate of spray in the specific volume
n	number density of liquid droplets
n_{vol}	number density of spherical obstacles
Nu	Nusselt number
q	heat flux
Q	volumetric heat flux
$\mathbf{r}$	radius vector of the droplet
R	radius of spherical obstacle
R_g	universal gas constant
S_d	specific surface area of liquid droplet
Stk	Stokes number ($= \rho_l d^2 u_0 / 18 \mu_g R$)
t	time
T	temperature
$\tilde{T}$	initial temperature within porous medium
u_0	velocity of gas flow
$\mathbf{v}$	velocity vector of inviscid flow
$\mathbf{V}$	dimensionless velocity vector of inviscid flow
x_d, y_d	dimensionless space coordinates of liquid droplet in Section 2.3
x_L	thickness of porous medium
y_{dc}	distance from the centerline of the flow to outermost trajectory of droplet which collides with obstacle.

Greek symbols

α	collision probability
α_d	collection efficiency of droplets on single obstacle
δ	Kronecker symbol
φ	polar angle
γ	volumetric heat transfer coefficient between different phases
ε	porosity of porous medium
ε_{vap}	effectiveness of evaporation
λ	thermal conductivity
μ	dynamic viscosity
θ	dimensionless time
ρ	density
τ	optical coordinate ($=kx$)
τ_c	optical thickness of porous medium ($=kx_L$)
ξ	dimensionless radius vector of the droplet.

Subscripts

0	initial
a	air
d	single droplet
g	gas phase
gl	between gas and liquid phases
gs	between gas and solid phases
f	fuel
l	liquid phase
r	radiation
s	solid phase
sat	saturation
sl	between solid and liquid phases
v	fuel vapor
vpr	evaporation product.

space, there are a few articles devoted to the interaction of surface of solid and the combustion of liquid fuel. Boyarshinov *et al.* [13] reported the experimental results of ethanol evaporation from a porous surface and its combustion in an air flow. Michaelides *et al.* studied droplet vaporization in a channel with constant wall temperature [14], and also under turbulent flow [15]. Howell *et al.* [16] pointed out that much less analysis has been published on liquid fuel combustion in porous media burners.

The main objective of the present work is to formulate a fundamental model to consider the evaporation and combustion of a fuel droplet mist in an inert porous medium. By extending the theoretical study on the phase change phenomenon inside the porous medium without combustion [17], we try to combine combustion and different heat transfer modes as well as the droplet behavior in the porous medium. Special interest is focused on self-sustaining combustion within the porous medium.

2. MATHEMATICAL MODELING

2.1. *Description of physical model*

Since the formulated subject of study incorporates so many phenomena, considerable simplification is necessary to make the physical model capable of fur-

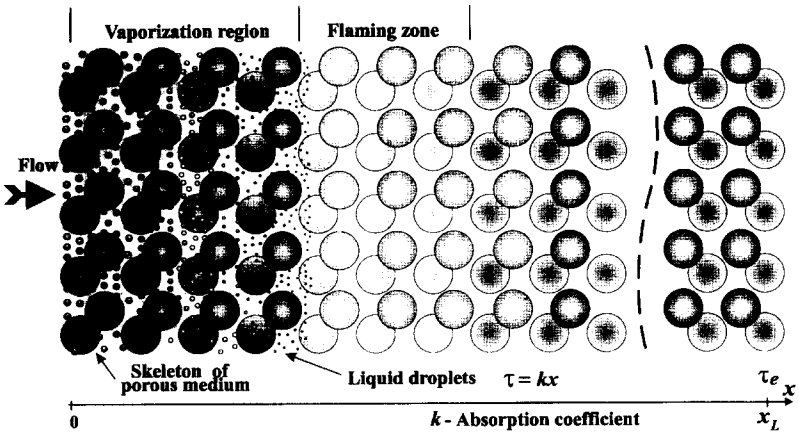

Fig. 1. Sketch of physical model.

ther numerical simulation. The proposed one-dimensional (1-D) model describes the interaction of the three considered phases: gas (air, vapor of fuel, and combustion products), fuel in liquid, and porous medium in solid. Schematically, the physical model is shown in Fig. 1. Fuel droplets are injected from nozzles and are evaporated by heat transfer originally from the flame located in the downstream within the porous medium. Although this combustion system should be first ignited by an external heat supply such as a preheated porous medium, self-sustaining combustion can be realized after ignition of relevant conditions are suitably adjusted.

The porous medium of high porosity is modeled by uniformly distributed spheres; moreover, there is uniform distribution of cavities with equal mean pore size in the porous medium. Since modern swirl nozzles are able to produce a mist of liquid droplets with mean diameter in the order of 10 μm, the behavior of droplets with initial diameter 10–50 μm is considered. Therefore, the average size of the fuel droplets is small enough compared to the average size of the pores. Liquid fuel droplets are monodisperse. The interaction between droplets during evaporation is neglected. Physical properties of fuel such as latent heat of evaporation and heating value are constant. Pseudo-steady-state conditions are assumed for the evaporation. The temperature distribution inside of the fuel droplet is uniform, but time-varying.

Basically actual applications with self-sustaining combustion are considered to be operated under relatively small rates of mass flow. Therefore, laminar isobaric flow consisting of air, fuel droplets, gaseous combustible mixture and hot products of combustion with constant velocity u_0 is assumed.

The evaporation gaseous fuel is assumed to be mixed immediately with air to form a homogeneous combustible mixture. Combustion is modeled using the Arrhenius approach for a single-step chemical reaction of a premixed flame with relevant kinetic constants of reactions from ref. [18]. Overall density and thermophysical properties of the gaseous phase are treated as constant. Mass fraction of the liquid is negligible, and the gas is optically transparent. Accordingly, radiative heat transfer between the skeleton surfaces of the porous medium is considered at the present stage. The radiative heat transfer around liquid droplets are not taken into account.

The most probable modes of heat exchange between different phases are shown in Fig. 2. It is assumed that the heat transfer between gas and solid is dominant. Also, the unidirectional characters of heat transfer from gas to liquid and from solid to liquid are suggested. The fraction of the convective heat transfer between gas–liquid and solid–liquid is described by parameter α, which is explained in Section 2.3 in detail. Because of the preheating of the solid and low heat capacity of gas, it is highly unlikely that the temperature of the liquid will be higher than that of the gas or solid.

On the basis of the above-mentioned assumptions, we solve the governing equations consisting of the energy conservation equations for the gaseous, solid and liquid phases. The basic framework of the following equations other than combustion, droplets motion and droplets heat transfer is similar to that in the previous paper [17].

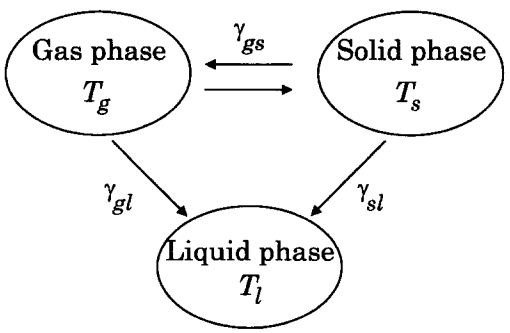

Fig. 2. Scheme of the most probable convective heat transfer modes between three phases: liquid, gas and solid.

2.2. *Mathematical formulation*

The 1-D governing equations are as follows.

Energy equation for gas phase.

$$\varepsilon\frac{\partial}{\partial t}[(c_a\rho_a+c_{vpr}\rho_{vpr})T_g]+\frac{\partial}{\partial x}[(c_a\rho_a+c_{vpr}\rho_{vpr})u_0T_g]$$

$$=\lambda_g\frac{\partial^2T_g}{\partial x^2}+\gamma_{gs}(T_s-T_g)-(1-\alpha)(1-\delta)\gamma_{gl}(T_g-T_l)$$

$$+\rho_v\cdot H\cdot A\cdot\exp\left(-\frac{E}{R_gT_g}\right)-(1-\alpha)\delta\dot{M}_fL \qquad (1)$$

where,

$$\rho_{vpr}\equiv\rho_{f0}-\rho_f$$

$$\delta=\begin{cases}0, & \text{for } T_l<T_{sat}\\ 1, & \text{for } T_l=T_{sat} \quad \text{and } T_g\geqslant T_{sat}\end{cases}$$

H is the combustion heat, L is the latent heat of evaporation, and T_{sat} is the saturation temperature of solvent–fuel mixture. The right-hand side terms of the equation describe thermal conduction, convective heat transfer among phases (gas–solid and gas–liquid), combustion, and vaporization, respectively.

Energy equation for solid phase.

$$c_s(1-\varepsilon)\rho_s\frac{\partial T_s}{\partial t}=-\gamma_{gs}(T_s-T_g)+\alpha(1-\delta)\gamma_{sl}(T_l-T_s)$$

$$+(1-\varepsilon)^2\lambda_s\frac{\partial^2T_s}{\partial x^2}-\frac{\partial q_r}{\partial x}-\alpha\delta\dot{M}_fL \qquad (2)$$

where the radiative term is written as follows

$$\frac{\partial q_r(\tau)}{\partial x}=-2\pi k\left[I_0E_2(\tau)+I_eE_2(\tau_c-\tau)-2I_b\right.$$

$$\left.+\int_0^{\tau_c}I_b(\tau')E_1(|\tau'-\tau|)\,d\tau'\right].$$

The Dulnev's expression for effective thermal conductivity of a solid $(1-\varepsilon)^2\lambda_s$ referred to in ref. [19] is used in the present formulation.

Energy equation for liquid phase.

$$\varepsilon c_l\frac{\partial}{\partial t}[\rho_fT_l]+c_l\frac{\partial}{\partial x}[\rho_fu_0T_l]$$

$$=(1-\alpha)(1-\delta)\gamma_{gl}(T_g-T_l)-\alpha(1-\delta)\gamma_{sl}(T_l-T_s) \qquad (3)$$

where $\rho_f=\rho_ln(\pi d^3/6)$; this equation is applicable only for the region $T_l\leqslant T_{sat}$.

Mass conservation equation for liquid phase.

$$\varepsilon\frac{\partial\rho_f}{\partial t}+\frac{\partial}{\partial x}[\rho_fu_0]=-\delta\cdot\dot{M}_f \qquad (4)$$

where

$$\dot{M}_f=\frac{(1-\alpha)\gamma_{gl}(T_g-T_{sat})+\alpha\gamma_{sl}(T_s-T_{sat})}{L+c_g(T_g-T_{sat})}. \qquad (5)$$

Equation (5) means that the total convective heat flux under constant saturation temperature of the liquid causes the evaporation of droplets and contributes to the change of the temperature of the gaseous phase.

Mass conservation equation for fuel vapor.

$$\varepsilon\frac{\partial\rho_v}{\partial t}+\frac{\partial}{\partial x}[\rho_vu_0]=\delta\cdot\dot{M}_f-\rho_v\cdot A\cdot\exp\left(-\frac{E}{R_gT_g}\right). \qquad (6)$$

Different modes of convective heat transfer are described by using the volumetric heat transfer coefficient γ. Assuming that both Nusselt numbers between of gas–solid and gas–liquid pairs $Nu_{gs}=h_{gs}D/\lambda_g$ and $Nu_{gl}=h_{gl}d/\lambda_g$ are equal to 2, the convective heat transfer coefficients per unit volume are defined as $\gamma_{gs}=(6\lambda_g/D^2)Nu_{gs}$, and $\gamma_{gl}=(\lambda_gNu_{gl}/d)S_d$, where S_d is a specific surface are of a liquid droplet. In the present model, heat transfer between liquid mist and solid phase is described by $\gamma_{sl}=h_{sl}S_d$, where h_{sl} is the heat transfer coefficient between the droplet and the solid, and is given in Section 2.4. The parameter α denotes the probability of the liquid droplet evaporating on a solid surface.

The computational domain is extended over the region upstream of the porous medium as well as the porous region in order to predict the gradient of the gas temperature in the region immediately upstream of the porous medium.

Initial and boundary conditions are given as follows:

$$\begin{aligned}
&T_l(-\infty,t)=T_0\\
&\rho_f(-\infty,t)=\rho_{f0}\\
&\rho_v(-\infty,t)=0\\
T_g(x,0)&=T_0 \qquad T_g(-\infty,t)=T_0\\
T_s(x,0)&=\tilde{T}(x) \qquad -\lambda_g\frac{\partial^2T_g(x_L,t)}{\partial x^2}=0\\
T_l(x,0)&=T_0\\
\rho_f(x,0)&=\rho_{f0} \qquad -(1-\varepsilon)^2\lambda_s\frac{\partial T_s(0,t)}{\partial x}\\
\rho_v(x,0)&=0 \qquad\quad =h_b[T_g(0,t)-T_s(0,t)]\\
&\qquad -(1-\varepsilon)^2\lambda_s\frac{\partial T_s(x_L,t)}{\partial x}=0
\end{aligned} \qquad (7)$$

2.3. *Description of liquid droplets motion and their collection on the skeleton of solid*

Variation of α in equations (1)–(3) and (6) within range [0, 1] allow us to simulate the different regimes of fuel vaporization. To improve understanding of the collision dynamics and to provide the most probable value of α, the model involving droplet impingement on the skeleton of the porous medium is suggested. The applied model is mainly based on the trajectory analysis of the droplets captured by immersed solid obstacle of simple shape [20]. As shown in Fig. 3, a trajectory of moving droplet follows the streamline of gas flow, but deviates from it in the neighborhood of the obstacle because of inertia. Depending on starting

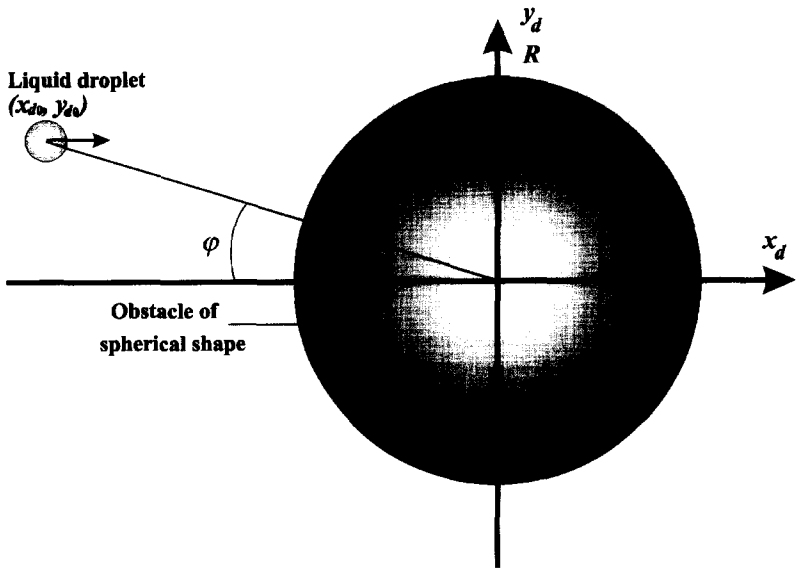

Fig. 3. Sketch of liquid droplet motion.

conditions, the droplet either is intercepted by an obstacle or moves away from it. If y_{dc} denotes the distance between the outermost trajectory for which the particles still collide with the obstacle and the centerline of the flow, collection efficiency of droplets on sphere is defined as $\alpha_d = (y_{dc}/R)^2$ [21].

Here, we assume that the interaction force of the droplet with the flow is only the ordinary Stokes drag, and we neglect the variation of the droplet diameter during the motion around a single obstacle. Consequently, the equation of droplet motion at $\mathbf{r}$ is written in the form of the second law of Newton:

$$\frac{\pi}{6} d^3 \rho_l \frac{\mathrm{d}^2\mathbf{r}}{\mathrm{d}t^2} = 3\pi\mu_g d\left(\mathbf{v} - \frac{\mathrm{d}\mathbf{r}}{\mathrm{d}t}\right). \tag{8}$$

Equation (8) can be rewritten in dimensionless form

$$Stk \frac{\mathrm{d}^2\boldsymbol{\xi}}{\mathrm{d}\theta^2} = \mathbf{V} - \frac{\mathrm{d}\boldsymbol{\xi}}{\mathrm{d}\theta} \tag{9}$$

using the following variables

$$\boldsymbol{\xi} = \frac{\mathbf{r}}{R} \quad \mathbf{V} = \frac{\mathbf{v}}{u_0} \quad \theta = \frac{u_0 t}{R} \quad Stk = \frac{\rho_l d^2 u_0}{18\mu_g R}. \tag{10}$$

In the case of inviscid flow around an obstacle of spherical shape, substituting explicit expression for the velocity component, equation (9) is rewritten for $x_d = \xi \cdot \cos\varphi$ and $y_d = \xi \cdot \sin\varphi$ projections, respectively [20]:

$$Stk \frac{\mathrm{d}^2 x_d}{\mathrm{d}\theta^2} = 1 - \frac{2x_d^2 - y_d^2}{2(x_d^2 + y_d^2)^{5/2}} - \frac{\mathrm{d}x_d}{\mathrm{d}\theta} \tag{11}$$

$$Stk \frac{\mathrm{d}^2 y_d}{\mathrm{d}\theta^2} = -\frac{3y_d x_d}{2(x_d^2 + y_d^2)^{5/2}} - \frac{\mathrm{d}y_d}{\mathrm{d}\theta}. \tag{12}$$

Required boundary conditions are written as follows:

$$x_d|_{t=0} = -\infty \quad y_d|_{t=0} = y_0$$

$$\left.\frac{\mathrm{d}x_{d0}}{\mathrm{d}t}\right|_{t=0} = u_0 \quad \left.\frac{\mathrm{d}y_{d0}}{\mathrm{d}t}\right|_{t=0} = 0. \tag{13}$$

By increasing y_{d0} step by step, the critical value y_{dc} is obtained.

This model of deposition efficiency is extended for the case of manifold obstacles by the addition of some simple assumptions. In the case of a uniform distribution of solid spheres with equal distances between them, the volumetric number density of solid spheres is $n_{vol} = (1-\varepsilon)6/\pi D^3$. Consequently, the amount of solid spheres equaled to $n_{vol}^{1/3} = [(1-\varepsilon)6/\pi]^{1/3}/D$ are disposed equidistantly. We may consider the spheres as a single obstacle with character size $[(1-\varepsilon)6/\pi]^{1/3}$. Accordingly the collision probability within one pore is

$$\alpha = \alpha_d \cdot [(1-\varepsilon)6/\pi]^{1/3}. \tag{14}$$

2.4. *The estimation of heat transfer coefficient between liquid and solid*

The assumptions for the derivation of heat transfer coefficient between liquid and solid are based on the results given by Ganic and Rohsenow [22]. They summarized experimental data of the effectiveness of evaporation ε_{vap} presented by different investigators. Also, they tried to fit these data by the simple analytical expression based on wall T_w and saturation T_{sat} temperature:

$$\varepsilon_{vap} = \exp\left[1 - \left(\frac{T_w}{T_{sat}}\right)^m\right]. \tag{15}$$

The expression (15) for ε_{vap} with $m = 2$ passes through the middle of the scattered experimental data. Because of this, the following formula for specific heat transfer from the solid to the liquid droplets is used in the present study

$$q_{sl} = u_0 \rho_l L \cdot \exp\left[1 - \left(\frac{T_w}{T_{sat}}\right)^2\right]. \quad (16)$$

Thus, heat transfer coefficient between solid and liquid is

$$h_{sl} = q_{sl}/(T_s - T_l). \quad (17)$$

2.5. *The computational technique*

The solutions to the system of coupled heat and mass transfer problems in equations (1)–(4) and (6) with initial and boundary conditions (7) are obtained numerically using finite differences. The governing equations are discretized into algebraic equations by using the control volume method. The gradients of the functions are stated in backward difference.

A predictor–corrector method scheme of fourth-order is used with Richardson extrapolation during the predictor step. For reducing computational time the technique of adaptive time step is applied. Also a non-staggered space mesh is used with maximum space step $0.01 \cdot x_L$. The finer meshes are set at the entrance region, and combustion and vaporization zones within the porous medium. Re-meshing is carried out when combustion and/or vaporization fronts change their position. Time increment is adjusted during computational procedure in order to minimize amount of iterations on every time step. To ensure the validity of the numerical scheme, the test calculations are performed, in particular the limiting case of gaseous premixed combustion without vaporization. Numerically obtained radiative heat flux distribution is compared with published computational results of high temperature gas flow without phase change [23] Also the overall energy and mass balance is calculated to check accuracy of computations. A steady-state solution is obtained when the mass and energy imbalance becomes less than 0.5 and 1%, respectively.

3. RESULTS AND DISCUSSION

3.1. *Behavior of liquid droplets*

Prior to the discussion on thermal and reaction characteristics of the system, the fluid dynamics of liquid droplets is of primary importance. The system of equations (11)–(13) is solved numerically under different values of Stokes number. Predicted trajectories of liquid droplets with streamlines of inviscid flow are shown in Fig. 4 under $Stk = 1$. The value of y_{dc} is equal to 0.67. Since the maximum value of Stk is about 4 under the postulated condition ($d = 50$ μm, $R = 150$ μm, $u_0 = 0.1$ m s^{-1}), Fig. 5 shows the variation of α_d for $Stk = 4$. The computational results are fixed are fitted well by the following polynomial equation using a least-square method for Stk within range $[0.5 \div 4]$:

$$\alpha_d = 0.093 + 0.387 \cdot Stk - 0.054 \cdot Stk^2. \quad (18)$$

Therefore, we can rewrite equation (14) in the form

$$\alpha = \left[\frac{(1-\varepsilon)6}{\pi}\right]^{1/3} \cdot (0.093 + 0.387 \cdot Stk - 0.054 \cdot Stk^2). \quad (19)$$

3.2. *Typical result of stable self-sustaining combustion*

In order to check the applicability of the computational model described in Chapter 2, a number of the numerical calculations have been done by widely changing the principle parameters. As a result, a steady solution corresponding to the stable self-sustaining combustion of fuel vapor is obtained. A general discussion for a variety of the relevant parameters, however, is very difficult, because of difficulty to stabilize the flame zone within the porous medium.

Hence, a typical result corresponding to the steady solution is shown in Fig. 6, under the operating conditions listed in Table 1. There are three temperature distributions, mass fraction profiles of liquid phase and combustible vapor, and reaction rate. The ambient temperature is used to normalize the temperature of each phase. The mass fractions of liquid and fuel vapor are normalized on the initial mass fraction of liquid. The amount of liquid diminishes by evaporation only and the mass fraction of gaseous fuel increases in the vaporization region and quickly vanishes by combustion. The differences between solid and gas temperatures is small except in the flame zone. The distributions of volumetric heat fluxes and evaporation rate are shown in Fig. 7. At the entrance region evaporation is governed by the heat transfer between the solid and liquid phases. With increasing x, however, the collision probability α decreases owing to the decrease of the droplets diameter d; as a result

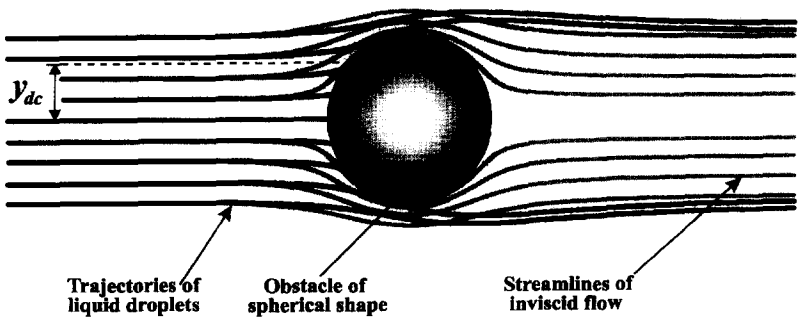

Fig. 4. Streamlines of inviscid flow and trajectories of liquid droplets around spherical obstacle.

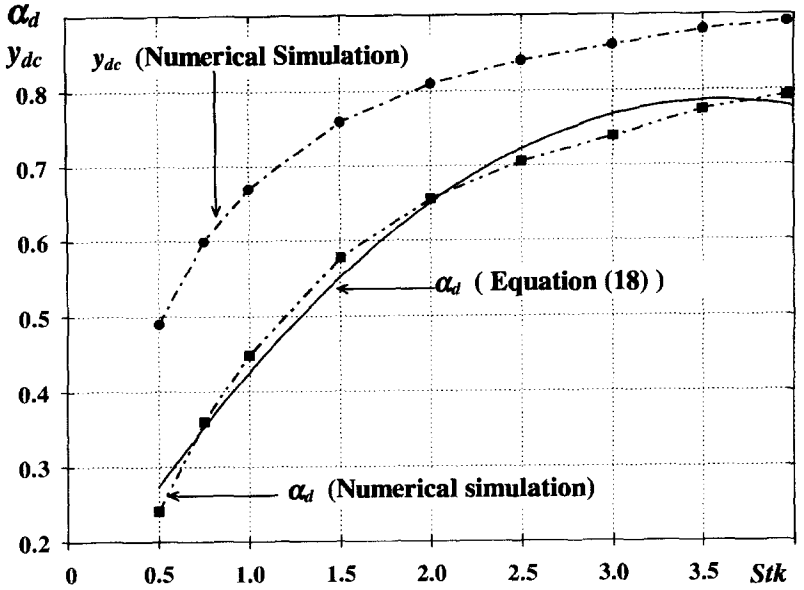

Fig. 5. Calculated deposition efficiency for single obstacle of spherical shape.

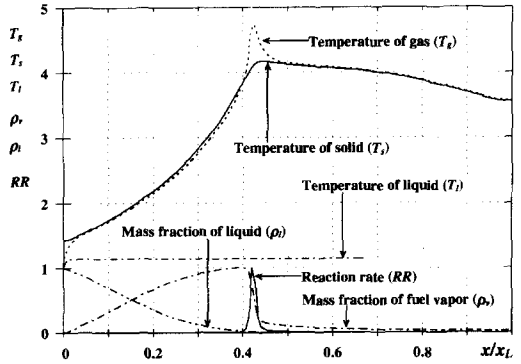

Fig. 6. Calculated temperature and mass fraction distributions within porous medium.

Table 1. Computational parameters

Frequency factor	A	$3.38 \cdot 10^{11}$	s^{-1}
Specific heat of gas	c_g	1200	$J\,kg^{-1}\,K^{-1}$
Specific heat of solid	c_s	1500	$J\,kg^{-1}\,K^{-1}$
Specific heat of liquid	c_l	3010	$J\,kg^{-1}\,K^{-1}$
Initial diameter of liquid droplet	d_0	25	μm
Mean size of element of porous material structure	D	300	μm
Activation energy	E	$2.3 \cdot 10^5$	$J\,mol^{-1}$
Combustion heat	H	$18.2 \cdot 10^6$	$J\,kg^{-1}$
Latent heat of evaporation	L	$1.3 \cdot 10^6$	$J\,kg^{-1}$
Universal gas constant	R_g	8.314	$J\,mol^{-1}\,K^{-1}$
Initial temperature	T_0	300	K
Saturation temperature	T_{sat}	341	K
Velocity of gas flow	u_0	0.1	$m\,s^{-1}$
Porosity of porous medium	ε	0.9	
Thermal conductivity of gas	λ_g	0.03	$W\,(m\,K)^{-1}$
Thermal conductivity of solid	λ_s	35	$W\,(m\,K)^{-1}$
Density of solid	ρ_s	800	$kg\,m^{-3}$
Density of liquid	ρ_l	853	$kg\,m^{-3}$
Optical thickness	τ_e	7.5	

the heat transfer between gas and liquid dominates at the final stage of evaporation.

The distributions of the heat fluxes are shown in Fig. 8. Convective heat flux is dominant in the whole computational domain. Under optical thickness $\tau_e = 7.5$, radiative flux also plays an important role. The conductive heat flux of gas is almost negligible in our system except in the flame zone. On the contrary, conductive heat flux of solid is considerable in the preheating region and achieves its maximum in the vicinity of the flame.

3.3. *Comparison with available experimental results*

Though there are very few works devoted to this topic, some experimental results are available for comparison. The simulation is carried out for the geometric parameters and thermophysical properties available from experimental results by Kaplan and Hall [24]. Their experiment was carried out on combustion of liquid droplets with initial diameter $d_0 = 50$

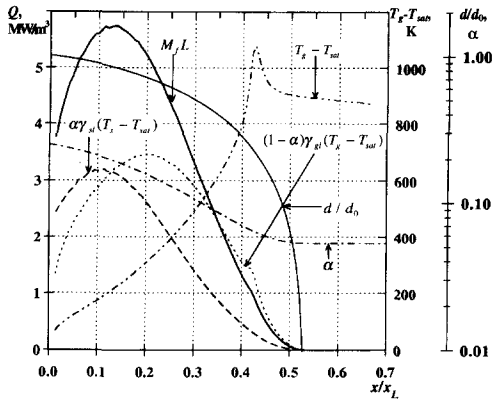

Fig. 7. Distribution of the temperature difference $T_g - T_{sat}$, volumetric heat fluxes Q, mean diameter of liquid droplets d/d_0 and collision probability α vs dimensionless coordinate x/x_L in evaporation region.

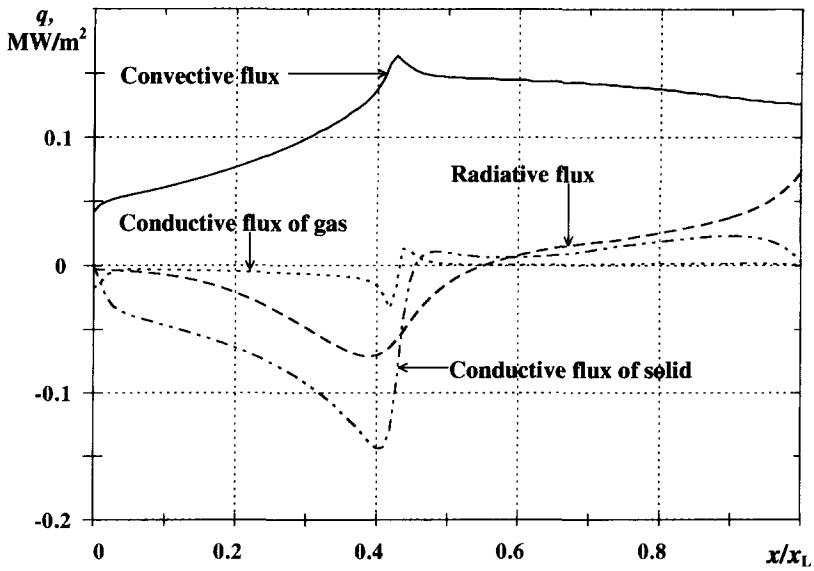

Fig. 8. Calculated heat flux distribution within porous medium.

μm within a magnesia-stabilized zirconia burner. Several configurations of 4-ppcm and 10-ppcm were used in the experimental device. The stable combustion was achieved under mean velocity of the flow through ceramic, about 0.75 m s^{-1}, within the range of equivalence ratio 0.57–0.67. The calculated temperature profile and measured axial temperature distributions along the combustion section of the porous ceramic burner at equivalence ratio 0.64 are plotted in Fig. 9. It can be seen that good agreement between the present theory and the experiment is achieved everywhere except at the entrance region of the combustion zone. The predicted steep temperature gradient in the entrance is associated with the vaporization process.

3.4. *Limitations of present model and future work*

Since the mathematical model is simplified considerably, the present model is valid within a relatively narrow range of geometrical parameters. As has been emphasized by Kaplan and Hall [24] and Howell *et al.* [17], much work remains to be done to further investigate the combustion of liquid fuels on porous media. In particular, the effects of solid-phase properties and fluid-phase mixing and diffusion must be elucidated. On the other hand, the vaporization of liquid by radiation has to be considered in the entrance region of the porous medium. Also, the dynamics of the droplets and their accumulation in the pre-evaporation region has to be considered in detail.

4. CONCLUSIONS

A physical model of self-sustaining combustion of the gaseous mixture with simultaneous evaporation of fuel droplets in the porous medium is developed taking the droplet behavior during the collision into account. The regime of self-sustaining combustion with steady flame zone is found numerically. The prediction of the mathematical model are found in good agreement with the available experimental result.

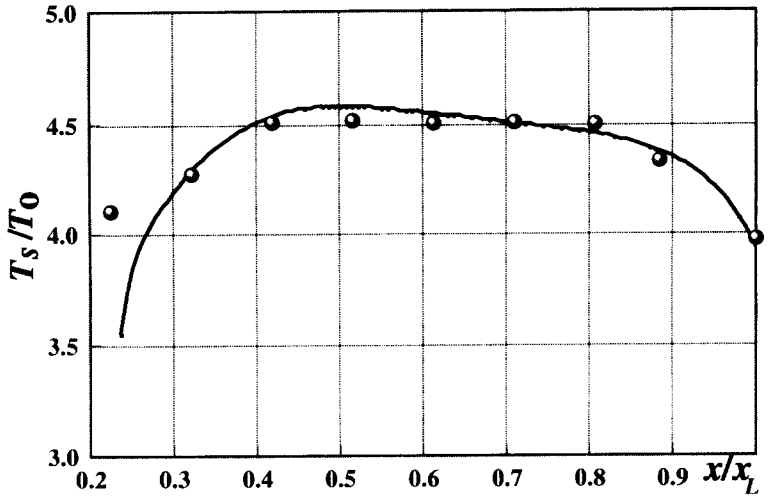

Fig. 9. Temperature distribution along combustion section: (●) experimental data from ref. [24], (—) numerical simulation.

The premixed combustion of fuel vapor in inert porous medium depends on various heat transfer modes. Although only the typical results were shown in the present paper, it is found that, under a fixed thickness of porous medium, the superficial velocity of the gaseous phase, thermal conductivity of the solid, convective heat transfer coefficients among different phases and initial diameter of liquid droplets are the most important parameters for self-sustaining combustion of the fuel vapor in an inert porous medium.

Acknowledgements—The present research was partially sponsored by the Ministry of Education, Science and Culture of Japan. The authors would like to express their thanks to Professor K. Kamiuto from Oita University, who made helpful comments on this work. The first author would also like to acknowledge the Ministry of Education, Science and Culture of Japan for his financial support.

REFERENCES

1. Weinberg, F. J., The first half million gears of combustion research and today's burning problems. *Proceedings of the Fifteenth International Symposium on Combustion*. The Combustion Institute, Pittsburg, 1975, pp. 1–17.
2. Jones, A. S., Lloyd, S. A. and Weinberg, F. J., Combustion in heat exchangers. *Proceedings of the Royal Society London*, 1978, **A360,** 97–115.
3. Echigo, R., Radiation enhanced/controlled phenomena of heat and mass transfer in porous media. *Proceedings* 1991 *ASME-JSME Thermal Engineering Joint Conference*, Vol. 4, 1991, pp. 21–32.
4. Babkin, V. S., Korzhavin, A. A. and Bunev, V. A., Propagation of premixed gaseous explosion flames in porous media. *Combustion and Flame*, 1991, **87,** 182–190.
5. Hanamura, K., Echigo, R. and Zhdanok, S. A., Superadiabatic combustion in a porous medium. *International Journal of Heat and Mass Transfer*, 1993, **36,** 3201–3209.
6. Zhdanok, S. A., Martynenko, V. V. and Shabunya, S. I., Obtaining superadiabatic temperatures in combustion of gaseous fuel in a system of two porous plates with a periodic change of the direction of pumping. *Journal of Engineering Physics and Thermophysics*, 1993, **64**(5), 463–469.
7. Commercial report, A new method of destroying organic pollutants in exhaust air. ADTEC Co., LTD, Sweden, 1990.
8. Echigo, R., Tawata, K., Yoshida, H. and Tada, S., Effective heating/cooling method for porous thermoelectric device in reciprocating flow combustion system. *Proceedings of* 1995 *ASME-JSME Thermal Engineering Joint Conference*, Vol. 4, 1995, pp. 389–396.
9. Hoffmann, J. G., Echigo, R., Tada, S. and Yoshida, H., Analytical study on flammable limits of reciprocating superadiabatic combustion in porous media. *Transport Phenomena in Combustion*, Vol. 2. Taylor & Francis, London, 1996, pp. 1430–1440.
10. Aggarwal, S. K., Tong, A. Y. and Siringano, W. A., A comparison of vaporization models in spray calculations. *AIAA Journal*, 1984, **22,** 1448–1457.
11. Abramzon, B. and Siringano, W. A., Droplet vaporization model for spray combustion calculations. *International Journal of Heat and Mass Transfer*, 1989, **32,** 1605–1617.
12. Elperin, T. and Krasovitov, B., Radiation, thermal diffusion and kinetic effects in evaporation and combustion of large and moderate size fuel droplets. *International Journal of Heat and Mass Transfer*, 1995, **38,** 409–418.
13. Boyarshinov, B. F., Volchkov, E. P. and Terekhov, V. I., Heat and mass transfer in a boundary layer with the evaporation and combustion of ethanol. *Combustion, Explosion and Shock Waves*, 1994, **30,** 7–13.
14. Michaelides, E. E. and Lasek, A., Particulate flow with sublimation or evaporation and with thermal and hydrodynamic non-equilibrium. *International Journal of Heat and Mass Transfer*, 1991, **34,** 601–609.
15. Michaelides, E. E., Liang, Li and Lasek, A., The effect of turbulence on the phase change of droplets and particles under non-equilibrium conditions. *International Journal of Heat and Mass Transfer*, 1992, **35,** 2069–2076.
16. Howell, J. R., Hall, M. J. and Ellzey, J. L., Combustion within porous inert media. Heat transfer in porous media and two-phase flow. *Energy and Environmental Expo '95, the Energy-Sources Technology Conference and Exhibition*, Houston, TX, ASME, HTD-Vol. 302, 1995, pp. 1–27.
17. Echigo, R., Yoshida, H. and Yun, J. H., Transient heat and mass transfer with condensable vapor in porous media. *Proceedings of the Tenth International Heat Transfer Conference*, Brighton, U.K., Vol. 5, 1994, pp. 231–236.

18. Aronowitz, D., Santoro, R. J., Dryer, F. L. and Glassman, I., Kinetics of the oxidation of methanol: experimental result semi-global modeling and mechanistic concepts. *Proceedings of the Seventeenth International Symposium on Combustion*. The Combustion Institute, Pittsburg, 1978, pp. 633–643.
19. Viskanta, R., Modeling of transport phenomena in porous media using a two-energy equation model. *Proceedings of* 1995 *ASME–JSME Thermal Engineering Joint Conference*, Vol. 3, 1995, pp. 11–22.
20. Buyevich, Yu. A. and Mankevich, V. N., Interaction of a dilute mist flow with a hot body. *International Journal of Heat and Mass Transfer*, 1995, **38,** 731–744.
21. Fuchs, N. A., *Mechanics of Aerosols*. Pergamon, New York, 1964, p. 140.
22. Ganich, E. N. and Rohsenow, W. M., Dispersed flow heat transfer. *International Journal of Heat and Mass Transfer*, 1977, **20,** 855–866.
23. Yoshida, H., Yun, J. H., Echigo, R. and Tomimura, T., Transient characteristics of combined conduction, convection and radiation heat transfer in porous media. *International Journal of Heat and Mass Transfer*, 1990, **33,** 847–857.
24. Kaplan, M. and Hall, M. J., The combustion of liquid fuels within a porous media radiant burner. *Experimental Thermal and Fluid Science*, 1995, **11,** 13–20.